cancer biology & therapy

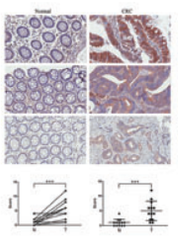

Cancer Biology & Therapy

ISSN: 1538-4047 (Print) 1555-8576 (Online) Journal homepage: https://www.tandfonline.com/loi/kcbt20

Strigolactone analogs act as new anti-cancer agents in inhibition of breast cancer in xenograft model

Einav Mayzlish-Gati, Dana Laufer, Christopher F Grivas, Julia Shaknof, Amiram Sananes, Ariel Bier, Shani Ben-Harosh, Eduard Belausov, Michael D Johnson, Emma Artuso, Oshrat Levi, Ola Genin, Cristina Prandi, Isam Khalaila, Mark Pines, Ronit I Yarden, Yoram Kapulnik & Hinanit Koltai

To cite this article: Einav Mayzlish-Gati, Dana Laufer, Christopher F Grivas, Julia Shaknof, Amiram Sananes, Ariel Bier, Shani Ben-Harosh, Eduard Belausov, Michael D Johnson, Emma Artuso, Oshrat Levi, Ola Genin, Cristina Prandi, Isam Khalaila, Mark Pines, Ronit I Yarden, Yoram Kapulnik & Hinanit Koltai (2015) Strigolactone analogs act as new anti-cancer agents in inhibition of breast cancer in xenograft model, Cancer Biology & Therapy, 16:11, 1682-1688, DOI: 10.1080/15384047.2015.1070982

To link to this article: https://doi.org/10.1080/15384047.2015.1070982

View supplementary material

Published online: 19 Oct 2015.

Submit your article to this journal

Article views: 884

View related articles

View Crossmark data

Citing articles: 24 View citing articles

Full Terms & Conditions of access and use can be found at
https://www.tandfonline.com/action/journalInformation?journalCode=kcbt20

RESEARCH PAPER

Cancer Biology & Therapy 16:11, 1682–1688; November 2015; © 2015 Taylor & Francis Group, LLC

Strigolactone analogs act as new anti-cancer agents in inhibition of breast cancer in xenograft model

Einav Mayzlish-Gati[1], Dana Laufer[1,2], Christopher F Grivas[3], Julia Shaknof[1], Amiram Sananes[1,2], Ariel Bier[1], Shani Ben-Harosh[2], Eduard Belausov[1], Michael D Johnson[4,5], Emma Artuso[6], Oshrat Levi[7], Ola Genin[7], Cristina Prandi[6], Isam Khalaila[2], Mark Pines[7], Ronit I Yarden[3,5], Yoram Kapulnik[1], and Hinanit Koltai[1,*]

[1]Institute of Plant Sciences; ARO; Volcani Center; Bet Dagan, Israel; [2]Faculty of Engineering Sciences; The Avram and Stella Goldstein-Goren Department of Biotechnology Engineering; Ben-Gurion University of the Negev; Beer-Sheva, Israel; [3]Department of Human Science; SNHS; Georgetown University; Washington, DC USA; [4]Department of Oncology; Georgetown University Medical Center; Washington, DC USA; [5]The Lombardi Comprehensive Cancer Center; Georgetown University Medical Center; Washington, DC USA; [6]Department of Chemistry; University of Turin; Torino, Italy; [7]Institute of Animal Sciences; Volcani Center; Bet Dagan, Israel

Keywords: breast cancer, cell motility, microtubule, plant hormone, strigolactone, xenograft

Abbreviations: SLs, strigolactones.

Strigolactones (SLs) are a novel class of plant hormones. Previously, we found that analogs of SLs induce growth arrest and apoptosis in breast cancer cell lines. These compounds also inhibited the growth of breast cancer stem cell enriched-mammospheres with increased potency. Furthermore, strigolactone analogs inhibited growth and survival of colon, lung, prostate, melanoma, osteosarcoma and leukemia cancer cell lines. To further examine the anti-cancer activity of SLs *in vivo*, we have examined their effects on growth and viability of MDA-MB-231 tumor xenografts model either alone or in combination with paclitaxel. We show that strigolactone act as new anti-cancer agents in inhibition of breast cancer in xenograft model. In addition we show that SLs affect the integrity of the microtubule network and therefore may inhibit the migratory phenotype of the highly invasive breast cancer cell lines that were examined.

Introduction

Acquired or pre-existing resistance to therapy is a major contributing factor for cancer treatment failure. Current hormonal or chemotherapy modalities often result in initial favorable response but ultimately, poor tolerance, adverse effects and resistance lead to the unsuccessful elimination of tumor cells and to local or distant disease relapse. Metastatic disease is the main cause of cancer-related death.

Therefore, there is an ever-increasing need for development of safe drugs and novel therapeutic strategies that target both the highly proliferating cells as well as the slow-growing cancer cells in an irreversible manner without harming the normal cells.

Multiple plant hormones (phytohormones) including Cytokinins, Methyl Jasmonate and Brassinosteroids are known as effective anti-cancer agents.[1] Strigolactones (SLs) are a novel class of plant hormones[2,3] that are produced by a wide variety of plant species.[4] A single plant species may produce several different isoforms of SLs but variation in combination of types and quantities of the different SLs may exist among the different members of a species. The SL structure consists of an ABC-ring system connected via an enol ether bridge to a butenolide D ring.[4] Currently about 17 natural SL were identified and more than 35 synthetic analogs have been synthesized and used in plant studies.[5,6]

Previously, we have shown that synthetic SL analogs induce growth arrest and apoptosis in breast cancer cell lines. We have shown that these compounds also inhibit the growth of breast cancer stem cell enriched-mammospheres with increased potency (Supplementary Table 1).[7] The synthetic analogs, MEB55 and ST362, used in the previous and the current studies have an indolyl based structure with a classical enol ether bridge connecting the C and D ring. The compounds are then further functionalized on the A ring with a thiophene ring in MEB55 and dioxathiophene in ST362 respectively. MEB55 is used as a racemic mixture (they differs for the configuration of C-2′ of the D ring) whereas ST362 as a diasteromeric mixture (an additional stereocenter is present on the C ring).[6]

SL analogs treatment of cancer cell lines is associated with down-regulation of cyclin B1, which was partially reversible in the presence of proteasome inhibitors and upon SLs removal. In addition, SL analogs activate the stress activated MAPKs, P38 and JNK1/2 and inhibit the activity of the survival factors: ERK1/2 and AKT.[7] SL analogs also inhibit growth and survival of colon, lung, prostate, melanoma, osteosarcoma and leukemia cancer cell lines.[8] The treatments with SLs result in the induction

*Correspondence to: Hinanit Koltai; Email: hkoltai@agri.gov.il
Submitted: 01/05/2015; Revised: 06/15/2015; Accepted: 07/03/2015
http://dx.doi.org/10.1080/15384047.2015.1070982

of G2 arrest, increased apoptosis, and loss of cells' viability. It was suggested that SL analogs affect different cell types by similar mechanisms, positioning them as novel broad-spectrum anti-cancer agents.[8]

To further characterize the anti-cancer activity of SL analogs, we have examined their effects alone and in combination with paclitaxel on growth of the breast cancer cell line, MDA-MB-231, in culture and as xenograft model. The results substantiated SLs activity as anti-cancer agents of MDA-MB-231 breast cancer tumors. A further insight into the mechanism of SLs activity suggests that like paclitaxel, treatment with SLs leads to an effect on the integrity of the microtubule network and to inhibition of cell migration.

Results

MEB55 has low toxicity in mice

MEB55 was administrated to mice at 12.5, 25, 50, 100 and 150 mg/kg. No differences were observed in mice body weight (BW) at all concentrations tested by either 8 or 14 d after the beginning of the treatment relative to the untreated controls (**Fig. 1A**). Liver sections stained with H&E indicated no histological changes up to 100 mg/kg while some abnormalities were observed at 150 mg/kg (**Fig. 1B**). Apoptotic cells in liver sections were apparent from 50 mg/kg treatment (**Fig. 1C**) and an increase in macrophage presence in the liver sections was detected in mice treated with 50 mg/kg of MEB55 (**Fig. 1D**). No substantial toxicity effects were found in mice treated with MEB55 at a dose of 25 mg/kg. Therefore, this dose was chosen to be tested for efficacy against MDA-MB-231 xenografts in mice. Notably, since MEB55 and ST362 are similar in structure and have both an indolyl based structure with a classical enol ether bridge connecting the C and D ring,[6] no escalation dose was done for ST362 since results are expected to be similar.

MEB55 and ST362 inhibit breast cancer tumor growth in mice

Mice implanted with xenografts of MDA-MB-231 were examined for the effect of MEB55 on solid tumors. MEB55 (25 mg/kg) treatments led to reduction in tumor volume and to reduced tumor growth rate (**Fig. 2**). The post hoc analysis reveals that there are statistically significant differences between the tumor sizes in control and treatment (MEB55) groups at time points of 6, 11, 15, 18, 21, 24 d post injection (DPI) (**Fig. 2A**; **Tables S2–S4**). The interaction of treatment and time is statistically significant ($p = 0.0017$).

Similar results of reduction in tumor growth rate were also obtained for ST362 (25 mg/kg; **Fig. S1**). Tumor growth rate of ST362 treated nude mice was significantly lower than tumor growth rate in control mice, and was similar to that of paclitaxel treated mice (**Fig. S1**). At the end of the experiment, tumor weight of mice treated with MEB55, ST362 or paclitaxel were reduced by 47%, 49% and 68% respectively, compared to untreated control. BW of treated mice was not significantly affected by either MEB55 or ST362 treatments (**Fig. S2** and data not shown, respectively).

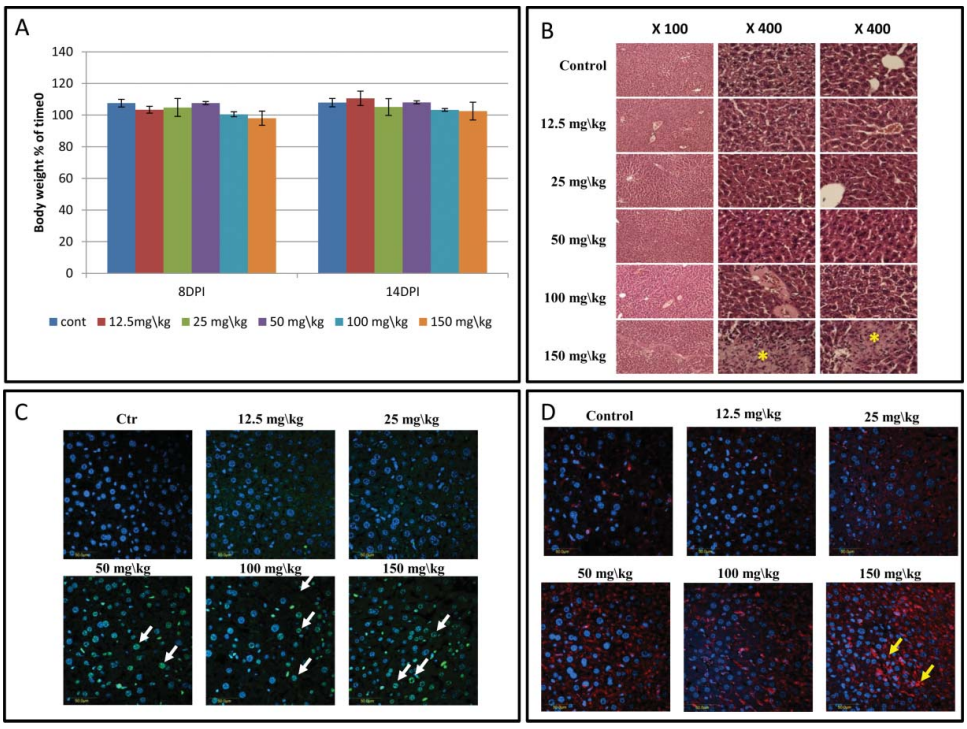

Figure 1. Results of toxicity experiment of MEB55 (12.5, 25, 50, 100 and 150 mg/kg) in Hsd:ICR(CD-1®) mice (n = 5 mice/treatment). Additional group was set as vehicle control. Mice were injected intraperitoneal (IP) twice a week with the MEB-55 solutions, dissolved with DMSO:Chromophor®EL 1:1 and diluted with double distilled water to the required concentration. (**A**) Body weight (% of time 0) at 8 and 14 d post injection (DPI). Values are means ± SE. (**B**) Hematoxylin and eosin (H&E) staining of liver sections. * - tissue abnormalities; pictures taken at different magnifications are shown (×100, ×400). (**C**) Apoptosis cell staining of liver sections using DeadEnd™ Fluorometric Tunnel system kit. White arrows point to the apoptic cells. (**D**) Immunostaining for macrophages of liver sections using polyclonal anti-macrophage antibodies (CL194P). Yellow arrows mark area of increase in macrophage presence.

MEB55 has an additive effect to that of paclitaxel in inhibition of growth and survival of breast cancer cell line

The effect of MEB55 in combination with paclitaxel was examined on the viability of MDA-MB-231 breast cancer cell line in culture.

Dose—effect curves were determined for each of the compounds and for concurrent treatments of MEB55 and paclitaxel (**Fig. 3**). For dose response assays, data points

were connected by non-linear regression lines of the sigmoidal dose-response relation. GraphPad Prism (version 6 for windows, GraphPad software Inc. San Diego, USA) was employed to produce dose-response curve and IC_{50} doses for SLs and paclitaxel by performing nonlinear regression analysis. In each case the upper limit was normalized to cell viability associated with treatment with the single, fixed-dose drug.

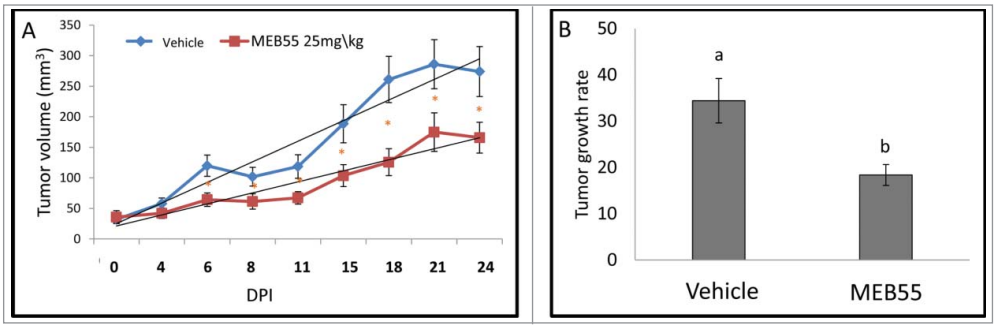

Figure 2. The effect of MEB55 (25 mg/kg) or vehicle treatments on xenografts of MDA-MB-231 in animal model of nude BALB/cOlaHsd-Foxn1nu mice. (**A**) Tumor volume (calculated as $V = \pi(\text{length}) \times (\text{width}) \times (\text{height})/6$) in mice treated with MEB55 (25 mg/kg) or vehicle; significant differences were analyzed by Wald test. * - Means are significantly different as determined by Student's-t-test ($P < 0.05$). (**B**) Tumor growth rate ($0.5 \times \text{small diameter}^2 \times \text{large diameter/day}$) in mice treated with MEB55 (25 mg/kg) or vehicle over DPI (days post injection). Values are means ± SE (n = 8); Different letters above the bars indicate statistically significant differences between means determined by Student's-t-test ($P \leq 0.05$).

Addition of paclitaxel to MDA-MB-231 cells resulted in a sigmoidal, concentration-dependent reduction in cell viability, with an IC_{50} of 16.87 nM (**Fig. 3A**). In the presence of 7.5 μM MEB55, MDA-MB-231 cells were sensitized to paclitaxel by 2.4 fold, i.e., IC_{50} of paclitaxel was 16.87 nM or 7 nM in the absence or presence of 7.5 μM MEB55, respectively (**Fig. 3A**). The enhanced sensitivity of MDA-MB-231 cells was noted only when cells were treated with paclitaxel at low concentrations (up to 25 nM after which levels of paclitaxel were too toxic to observe any additive activity).

Addition of MEB55 to MDA-MB-231 cells resulted in a sigmoidal, concentration-dependent reduction in cell viability, with an IC_{50} of 5.8 μM (**Fig. 3B**). Sensitivity of MDA-MB-231 cells to MEB55 was enhanced 2 fold when cells were co-treated with 10 nM paclitaxel, i.e., IC50 of MEB55 was 5.8 μM or 2.4 μM in the absence or presence of 10 nM paclitaxel, respectively (**Fig. 3B**). The additive effect of 10 nM paclitaxel was apparent at all MEB55 tested concentrations, up to 25 μM, which was the highest MEB55 concentration used. At this high concentration paclitaxel had no significant additive effect on MEB55 treatment.

Together, these results suggest an additive effect of paclitaxel and MEB55 on growth inhibition of MDA-MB-231 cancer cell growth.

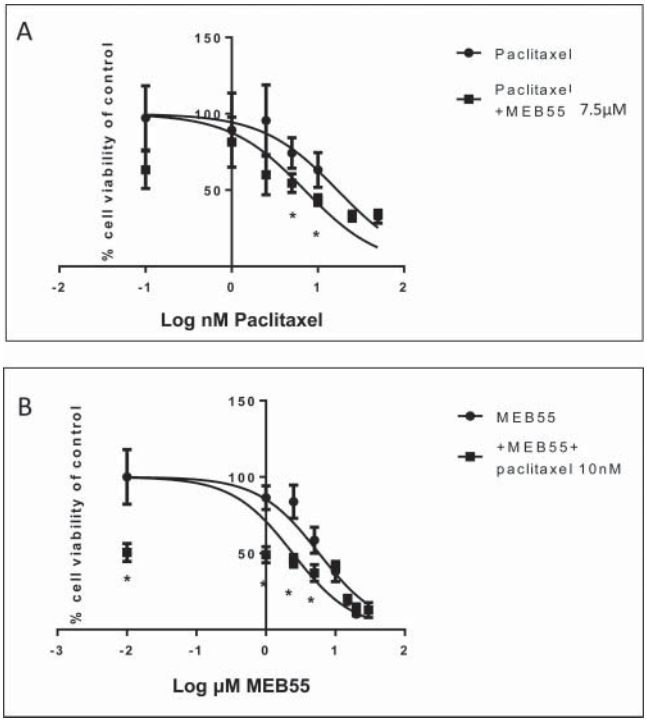

Figure 3. Dose response curves of MDA-MB-231 cell viability following treatment with MEB55 alone and in combination with paclitaxel. Cells were exposed to either single agent drug (**A**) paclitaxel or (**B**) MEB55 (circle) or to drugs combinations (**A**) paclitaxel + 7.5 μM of MEB55 or (**B**) Meb55 + 10 nM of paclitaxel (square) for 48 hours followed by XTT assay to determine cell viability. Cell survival (%) of control is calculated by = 100 × (At-Ac)(treatment) / (At-Ac)(control), where At and Ac are the absorbencies (450nm) of the XTT colorimetric reaction in treated and control cultures respectively minus non-specific absorption measured at 650nm. Data points are connected by non-linear regression lines of the sigmoidal dose-response relation. Values are means ± SE of 3 independent experiments. IC_{50} values were determined with nonlinear regression analysis. * Means are significantly different between single agent and combination as determined by Student's-t-test ($P \leq 0.05$).

Both MEB55 and paclitaxel act in inhibition of breast cancer tumor growth in animal model

Since MEB55 and paclitaxel showed an additive inhibitory effect on breast cancer cell line growth, we examined the combination of MEB55 and paclitaxel treatments on xenografts of breast cancer in mice. Mice were treated with either a low dose of paclitaxel: (7.5 mg/kg) or a high dose of paclitaxel (15 mg/kg). As expected, paclitaxel at a high dose significantly inhibited the growth of MDA-MB-231 xenograft tumors. MEB55 by itself or a lower dose of paclitaxel (7.5 mg/kg) were not as effective in retarding tumor growth. Concurrent administration of MEB55 and the low-dose of paclitaxel reduced to some extent, but not significantly, tumor volume compared to treatment with MEB55 only. Similarly, concurrent administration of MEB55 and the low-dose of paclitaxel reduced to some extent, but not significantly, tumor volume compared to treatment with low-dose of

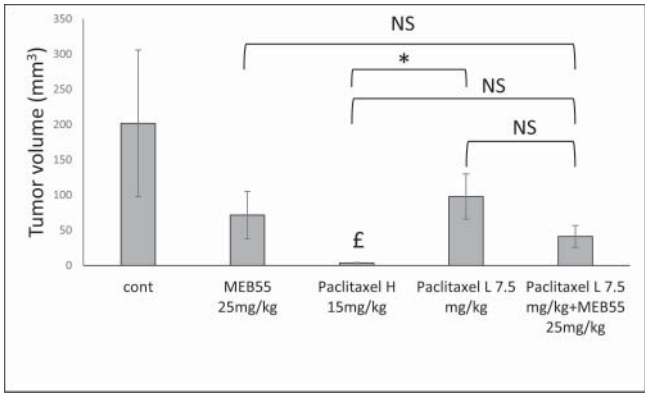

Figure 4. The effect of MEB55 (25 mg/kg; A) or paclitaxel in 2 concentrations (15 or 7.5 mg/kg) or combination of MEB (25 mg/kg) and paclitaxel (7.5 mg/kg) treatments on xenografts of MDA-MB-231 in animal model of nude BALB/cOlaHsd-Foxn1nu mice. Administration was by IP twice a week for 3 weeks. Tumor volume (mm^3; calculated as $V = \pi(\text{length}) \times (\text{width}) \times (\text{height})/6$) at the end of experiment (12 d post treatment initiation) is shown. Values are means ± SE (n = 8). *, Means are significantly different or NS, means are not-significantly different, as determined by Student's-t-test ($P \leq 0.05$). £, Treatment significantly different compared to control.

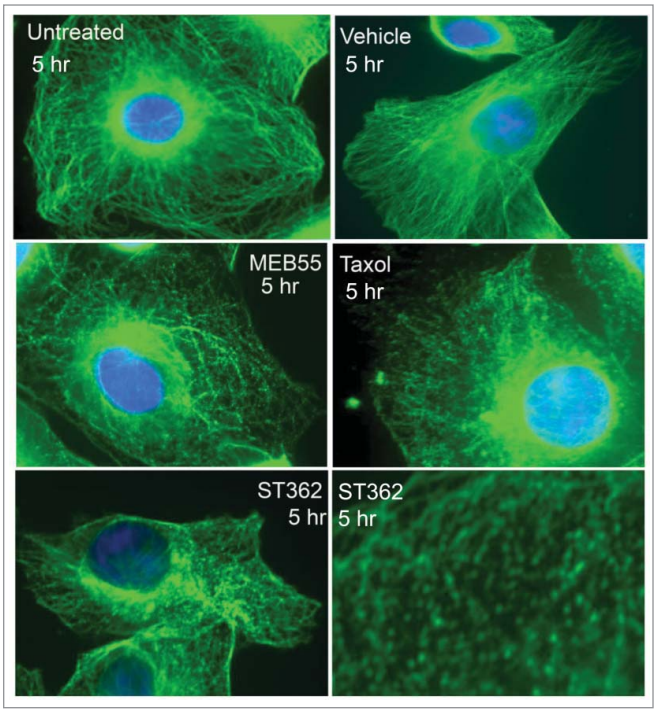

Figure 5. Fluorescent images of MDA-MB-231 cancer cells immunostained for α-tubulin (Green staining- Alexa Fluor 488) following MEB (15 μM), ST362 (15 μM), paclitaxel (Taxol, 2.5 nM), vehicle control treatments or untreated control for 5 hr. Blue nuclei staining- DAPI. Images were taken using Zeiss Axiovert 200M Fluorescense inverted microscope at ×630 magnification.

paclitaxel only. Also, only paclitaxel treatment at high dose was different from control. However, once MEB55 was administered concurrently with the low-dose of paclitaxel, tumor growth was significantly inhibited almost to the same extent as seen by administration of high-dose paclitaxel alone (**Fig. 4**; Student's t-test [$P \leq 0.05$]). However, since no statistically significant difference was found between MEB55 alone versus MEB55 and paclitaxel combined treatments, it cannot be concluded that MEB55 enhances the efficacy of paclitaxel alone on solid tumor growth.

MEB55 affects microtubule bundling and cell motility in breast cancer cells similarly to paclitaxel

To determine the effect of SLs on microtubules integrity, MDA-MB-231 cells were treated with 15 μM of MEB55 or ST362. Staining for α- tubulin demonstrated that MEB55 or ST362 lead to microtubule bundling, as soon as 5 hr after treatment (**Fig. 5**), suggesting that SLs affect the integrity of the microtubule network and therefore may inhibit the migratory phenotype of the highly invasive breast cancer cell lines: MDA-MB-231 and MDA-MB-436[9].

Using the *in vitro* scratch assay as described in Liang et al.,[10] a confluent monolayer of MDA-MB-231 (**Fig. 6**) or MDA-MB-436 (**Fig. S3**) cells was scratched and the ability of the cells to migrate into the scratch was examined in a time period of 24 h. For both MDA-MB-231 (**Fig. 6**) or MDA-MB-436 (**Fig. S3**), a marked reduction in the ability of the cells to migrate into the scratch was obtained for cells treated with MEB55 or ST362, similarly for those treated with paclitaxel, and in comparison to vehicle and non-treated control. Although cell count was reduced to some extent with the MEB55 and ST362 treatments in comparison to controls (**Fig. S4**), it may not fully account to the marked differences in cell migration observed between treatments and controls (**Fig. 6**). These results suggest that MEB55 and ST362 reduce MDA-MB-231 and MDA-MB-436 cell line migration, similarly to paclitaxel.

Discussion

We have previously shown that synthetic strigolactone analogs, including MEB55 and ST362, inhibit breast cancer cell growth and survival.[7] In the present study we show that these analogs are efficient in inhibiting growth of MDA-MB-231 xenograft tumors in animal model. Moreover, MEB55 at an effective concentration of 25 mg/kg caused only low level of toxicity, suggesting that it has the potential to be developed as an anti-cancer agent.

Furthermore, we have found that the concurrent administration of MEB55 and paclitaxel lead to an additive growth inhibition of MDA-MB-231 cultured cells. The additive effect was apparent only when the compounds were administrated at relatively low concentrations. At higher concentrations of MEB55 or paclitaxel, no additive effects were apparent between the 2 compounds in cultured cells. The additive effect obtained with concurrent administration of MEB55 and paclitaxel suggest that the 2 compounds affect cell proliferation by a similar mechanism. Therefore, at higher concentrations, the maximal effect of each

compound may mask the effect of the other compound. However, in xenograft model, treatment with MEB55 alone did not improve significantly tumor inhibition vs. MEB55 and paclitaxel combined treatment. Therefore, it cannot be concluded that MEB55 enhances the efficacy of paclitaxel on solid tumor growth.

We found that MEB55 and ST362 affect the integrity of the microtubules network. Within hours of treatment microtubule bundles are formed in the cytosol and around the cell nucleus. Interestingly, microtubules are the main target of paclitaxel in cells.[11,12] More specifically, paclitaxel was shown to successfully target class I and III β-tubulin,[13] and lead to straightening of the protofilaments, inducing a more GTP-like configuration in the microtubule protofilaments,[14,15] resulting with formation of microtubule bundles (**Fig. 5** and, e.g., Horwitz et al.,[11]). However, it is yet to be determined whether SLs are microtubules targeting agents.

Alterations in microtubule dynamics can influence cell migration via several different microtubule-dependent pathways.[16,17] Therefore, we have examined the effect of MEB55 on cell migration. In accordance with its effect on microtubules, MEB55 reduced the migration ability of 2 metastatic breast cancer cell lines: MDA-MB-231 and MDA-MB-436. Since cell migration was shown to be involved in metastasis formation (e.g., Jones et al.,[18]), these results may indicate that MEB55 may lead to reduced metastasis.

In summary, the SL analogs MEB55 and ST362 inhibit MDA-MB-231 tumor development in xenograft model. It would be of interest to determine whether SLs target microtubules directly. MEB55 relatively low toxicity and high efficacy suggest its usage as an anti-cancer agent to promote anti-cancer activity while reducing chemotherapy toxicity.

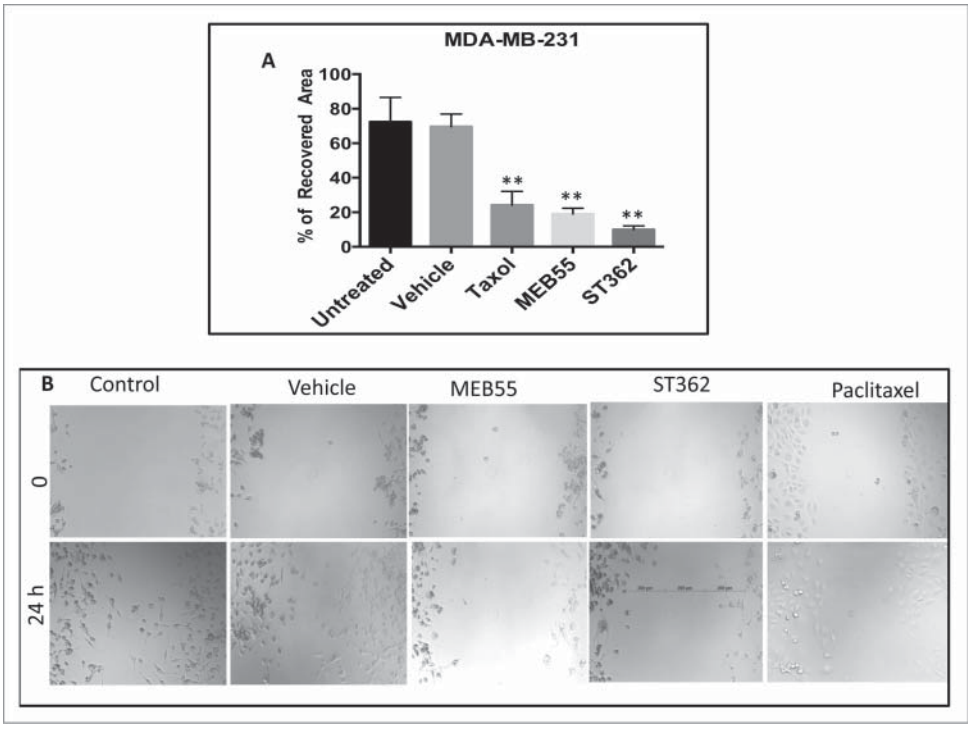

Figure 6. The effect of MEB55 (7.5 μM), ST362 (7.5 μM) or paclitaxel (Taxol, 2.5 nM), vehicle and untreated control on recovered area of confluent monolayers of MDA-MB-231 cancer cell line. Monolayer was scraped in a straight line and % recovered area of the scratch by cells that migrated into the scratch was measured from images taken at time 0 and 24 h and calculated as (0 h cell free area in treatment - 24 h cell free area in treatment)/ (0 h cell free area in untreated - 24 h cell free area in untreated) × 100. (A) Values are means ± SE (n = 8). *, Means are significantly different as determined by Student's-t-test. Paclitaxel and MEB55 treatments ($P < 0.0019$); ST362 treatment ($P < 0.0004$). (B) An example for the effect of MEB55 (7.5 μM), ST362 (7.5 μM) and paclitaxel (2.5 nM), vehicle and untreated control on recovered area of confluent monolayers of MDA-MB-231 cancer cell line cells in comparison to vehicle and untreated control. Bars demonstrate length of measurements.

Materials and Methods

Cell culture

Cells were grown at 37°C in a humidified 5% CO_2–95% air atmosphere. All tissue culture media and serum were purchased from Biological Industries LTD Israel, unless otherwise indicated. MDA-MB-231 (ATCC, Manassas, USA) were maintained in DMEM supplemented with 10% FCS, 1% Penicillin-Streptomycin Solution, and 1% L-glutamine. Viable cells were counted under a microscope by trypan blue (Sigma-Aldrich) exclusion.

Cell proliferation assay XTT base

Cells were seeded into a 96 well plates at 2,500 cells per well in triplicates in normal growing media. On the following day, the media was replaced with phenol red-free DMEM supplemented with 10% FBS (Foetal Bovine Serume) and 5% Penicillin-Streptomycin solution. Cells were incubated over night at 37°C in a humidified 5% CO_2–95% air atmosphere, and then were treated as indicated below for 48h. XTT (2, 3,-bis(2-methoxy-4-nitro-5-sulfophenyl)-5-[(phenylamino)-carbonyl]-2H-tetrazolium inner salt) reduction was used to quantify viability according to manufacturer's instruction (Biological industries, IL). Cells were incubated with XTT reagent for 2 h at 37°C in a humidified 5% CO2–95% air atmosphere. Absorbance was recorded by a VersaMax ELISA Microplate Reader (Molecular devises, USA) at 450 nm with 650 nm of reference wavelength. Cell survival was estimated from the equation: % cell survival of control = 100 × (At-Ac)(treatment) / (At-Ac)(control), where At and Ac are the absorbencies (450 nm) of the XTT colorimetric reaction in treated and control cultures respectively minus non-

specific absorption measured at 650 nm. Absorbance of medium alone was also deducted from specific readings. For dose response assays, data points were connected by non-linear regression lines of the sigmoidal dose-response relation.

Strigolactone analogs treatments

Strigolactone analogs MEB55 and ST362 (described above) were solubilized in DMSO (D2650; Sigma) at stock concentrations of 10 mM. Cells were treated at the indicated doses by diluting the analogs to the required highest concentration in the appropriate culture medium. Serial dilutions were performed for subsequent lower concentrations. At least 2 independent experiments were done for each treatment; in each experiment at least 3 technical replicates were performed.

Paclitaxel treatments

Paclitaxel (T7402; Sigma) was solubilized in DMSO at stock concentration of 10mM. Cells were treated at the indicated doses by dilution to the required highest concentration in the appropriate culture medium. Serial dilutions in culture medium were performed for subsequent lower concentrations. At least 2 independent experiments were done for each treatment; in each experiment at least 3 technical replicates were performed.

Cell migration studies

Cell motility assay was conducted as described in Liang et al.,[12] with several modifications. 1×10^6 to 1×10^4 MDA-MB-231 or MDA-MB-436 cells were seeded in each well of a 6 wells plate, in volume of 1 ml of growth medium. The cells were then spread throughout the well and allowed to adhere for 24 h. On the following day, the culture medium was then removed and replaced with a medium containing MEB55 treatment in 2 concentrations, or medium only for untreated control. In addition, cells were treated with DMSO as a vehicle control. Incubation was for another 24 h. Next, the medium was removed and the cells monolayer was scraped in a straight line using a 200 μl pipet tip to create a scratch. Debris were removed and the edges of the scratch were smoothed by washing the cells once with 1 ml of growth medium. Images of 3 marked points along the scratch in each well were taken with a phase-contrast microscope for time 0. Cells were incubated for additional 24 h in the presence of growth medium containing 1% FBS (to eliminate the possibility of cells filling the scratch by proliferation) and/or the indicated concentrations of MEB55 or with DMSO as vehicle control, and images of the same marked points in each well were again taken. Finally, images taken at time 0 and 24 h were compared and the cell free area was measured in each image using "IMAGEJ" software. % Recovered area, measured from the images, was calculated as (0 h cell free area in treatment - 24 h cell free area in treatment) / (0 h cell free area in untreated - 24 h cell free area in untreated) × 100. At least 2 independent experiments were done for each treatment; in each experiment at least 3 technical replicates were performed.

α tubulin staining

MDA-MB-231 cells were seeded on coverslips one day prior to treatments with the 2 analogs: MEB55 or ST362 for the indicated times. Cells were then fixed with 4% paraformaldehyde in 1X PBS and permeablized with 1% solution of Triton X-100 in 1X PBS. Untreated and vehicle-treated cells were fixed and stained as negative controls. For comparison, cells were treated with 2.5 nM of paclitaxel (Sigma). Following blocking with 10% Goat serum in PBS, cells were stained with a mouse monoclonal antibody against α-tubulin (A01410, Genescript Inc.) diluted 1:2000 in blocking buffer for 1 h at RT. The cells were washed 3 times for 5 minutes in 1X PBS. Cells were then incubated for 1 hour at room temperature in Rabbit anti mouse conjugated to Alexa Fluor 488 (Life Technologies) diluted 1:100 in blocking buffer. Cells were washed in 1X PBS 3 times for 5 minutes. Coverslips were mounted onto glass slides using mounting media and DAPI. Cells were visualized with Zeiss AxioVert 200M inverted Fluorescence microscope at × 63 magnification and ZeiessAxioCam, CCD camera.

Animal model experiments

Determination of strigolactone analogies toxicity

Mice Hsd:ICR(CD-1®((Harlen, Israel) were housed at a 12-hour light/12-hour dark cycle were treated with different concentrations of MEB-55, one of the most potent SL analog, in concentrations of 12.5, 25, 50, 100 and 150 mg/kg. Additional group was set as vehicle control (n = 5 mice/treatment). Mice were injected intraperitoneal (IP) twice a week with the MEB-55 solutions, dissolved with DMSO: Chromophor®EL 1:1 and diluted with double distilled water to the required concentration. Body weight (BW) was determined at times 0, 8 and 14 day post injection (DPI) of MEB55. At the end of the experiment, at 14 DPI, liver from control and treated mice were harvested, fixed with formalin and sectioned, as described below. All procedures were conducted in accordance to the institutional (IL-11–02–2012; IL-88–12–2012; IL 490/14) and national guidelines.

Determination of strigolactone analogs and paclitaxel effect on tumor growth

Mice BALB/cOlaHsd-Foxn1nu were implanted subcutaneous with 2×10^6 MDA-MB-231 cells. The tumors were allowed to grow until they reach an average of 35 mm^3 (about 2 weeks) and then mice were randomly assigned to the following groups (n = 8 mice/treatment). Experiment 1 consisted of the following treatments: (1) MEB55 (25 mg/kg); (2) vehicle control. Experiment 2 consisted of the following treatments: (1) ST362 (25 mg/kg); (2) paclitaxel (20 mg/kg); (3) vehicle control. Experiment 3 consisted of the following treatments: (1) paclitaxel (7.5 mg/kg); (2) paclitaxel (15 mg/kg); (3) MEB55 (25 mg/kg); (4) MEB55 (25 mg/kg) and paclitaxel (7.5 mg/kg). Administration was by IP twice a week for 3 weeks and mice survival and tumor volume were recorded. At the end of the experiments BW was determined prior to tumor harvest. Tumors volume was calculated as $V = \pi(\text{length}) \times (\text{width}) \times (\text{height})/6$.

Histological examination

Liver biopsies were fixed overnight in 4% paraformaldehyde in PBS at 4°C, embedded in paraffin 5-μm sections were prepared and stained with hematoxylin and eosin (H&E), For macrophages, determination, immunohistochemistry was performed using polyclonal anti-macrophage antibodies (CL194P; Acris, Hiddenhausen, Germany) at 1:250 dilution.[19] To evaluate the number apoptotic cells in the liver sections the DeadEnd™ Fluorometric Tunnel system kit (Promega) was used. This kit detects fragmental DNA of apoptotic cells.

Statistical Analyses

Results are presented as mean ± SE of replicate analyses and are either representative of, or inclusive of at least 2 independent experiments. Means of replicates were subjected to statistical analysis by Student's t-test ($P \leq 0.05$), using the JMP statistical package and regarded as being significant when $P \leq 0.05$ (*). GraphPad Prism (version 6 for windows, GraphPad software Inc. San Diego, USA) was employed to produce dose-response curve and IC_{50} doses for SLs and paclitaxel by performing nonlinear regression analysis. Tumor volume (0.5 × small diameter^2 × large diameter) was calculated and significant differences were analyzed by Wald test of tumor size change at different time points for mice in control and treatment groups ($P \leq 0.05$).

Disclosure of Potential Conflicts of Interest

No potential conflicts of interest were disclosed.

Acknowledgments

We thank Avner Levin, Moran Gelber and Peter Johnson for technical assistance, and Strigolab srl. for providing strigolactone analogs.

Funding

This research was partially funded by "Kamin" fund of The Israeli Ministry of Economy (HK and YK), The Chief Scientist Fund of The Israeli Ministry of Agriculture (IK), Georgetown SNHS research award (RIY) and Georgetown Undergraduate Research Opportunities Program, GUROP, (CFG). The immunefluorescence experiments were performed with advice and technical assistance of Microscopy and Imaging Shared Resource of the Lombardi Comprehensive Cancer Center partially supported by NIH/NCI grant P30-CA051008. Statistical analysis was provided by Dr. Hongkun Wang from the Georgetown University Biostatistics & Bioinformatics Shared Resource that is partially supported by NIH/NCI grant P30 CA051008 and GHUCCTS grant UL1 TR000101.

Supplemental Material

Supplemental data for this article can be accessed on the publisher's website.

References

1. Lin L, Tan RX. Cross-kingdom actions of phytohormones: a functional scaffold exploration. Chem Rev 2011; 111:2734-60; PMID:21250668; http://dx.doi.org/10.1021/cr100061j
2. Umehara M, Hanada A, Yoshida S, Akiyama K, Arite T, Takeda-Kamiya N, Magome H, Kamiya Y, Shirasu K, Yoneyama K, et al. Inhibition of shoot branching by new terpenoid plant hormones. Nature 2008; 455:195-200; PMID:18690207; http://dx.doi.org/10.1038/nature07272
3. Gomez-Roldan V, Fermas S, Brewer PB, Puech-Pages V, Dun EA, Pillot J-P, Letisse F, Matusova R, Danoun S, Portais J-C, et al. Strigolactone inhibition of shoot branching. Nature 2008; 455:189-94; PMID:18690209; http://dx.doi.org/10.1038/nature07271
4. Xie X, Yoneyama K, Yoneyama K. The Strigolactone Story. Ann Rev Phytopathol 2010; 48:93-117; PMID:20687831; http://dx.doi.org/10.1146/annurev-phyto-073009-114453
5. Zwanenburg B, Nayak SK, Charnikhova TV, Bouwmeester HJ. New strigolactone mimics: Structure–activity relationship and mode of action as germinating stimulants for parasitic weeds. Bioorg Med Chem Lett 2013; 23:5182-6; PMID:23920440; http://dx.doi.org/10.1016/j.bmcl.2013.07.004
6. Prandi C, Occhiato EG, Tabasso S, Bonfante P, Novero M, Scarpi D, Bova ME, Miletto I. New potent fluorescent analogues of strigolactones: synthesis and biological activity in parasitic weed germination and fungal branching. Eur J Organ Chem 2011; 2011:3781-93; http://dx.doi.org/10.1002/ejoc.201100616
7. Pollock C, Koltai H, Kapulnik Y, Prandi C, Yarden R. Strigolactones: a novel class of phytohormones that inhibit the growth and survival of breast cancer cells and breast cancer stem-like enriched mammosphere cells. Breast Cancer Res Treat 2012; 134:1041-55; PMID:22476848; http://dx.doi.org/10.1007/s10549-012-1992-x
8. Pollock CB, McDonough S, Wang VS, Lee H, Ringer L, Li X, Prandi C, Lee RJ, Feldman AS, Koltai H. Strigolactone analogues induce apoptosis through activation of p38 and the stress response pathway in cancer cell lines and in conditionally reprogramed primary prostate cancer cells. Oncotarget 2014; 5:1683-98; PMID:24742967
9. Sliva D, Rizzo MT, English D. Phosphatidylinositol 3-kinase and NF-κB regulate motility of invasive MDA-MB-231 human breast cancer cells by the secretion of urokinase-type plasminogen activator. J Biol Chem 2002; 277:3150-7; PMID:11689575; http://dx.doi.org/10.1074/jbc.M109579200
10. Liang C-C, Park AY, Guan J-L. In vitro scratch assay: a convenient and inexpensive method for analysis of cell migration in vitro. Nat Protoc 2007; 2:329-33; PMID:17406593; http://dx.doi.org/10.1038/nprot.2007.30
11. Horwitz SB, Cohen D, Rao S, Ringel I, Shen HJ, Yang CP. Taxol: mechanisms of action and resistance. J Natl Cancer Inst Monogr 1993:55-61; PMID:7912530
12. Carré M, Carles G, André N, Douillard S, Ciccolini J, Briand C, Braguer D. Involvement of microtubules and mitochondria in the antagonism of arsenic trioxide on paclitaxel-induced apoptosis. Biochem Pharmacol 2002; 63:1831-42; PMID:12034367; http://dx.doi.org/10.1016/S0006-2952(02)00922-X
13. Ferlini C, Raspaglio G, Mozzetti S, Cicchillitti L, Filippetti F, Gallo D, Fattorusso C, Campiani G, Scambia G. The seco-taxane IDN5390 is able to target class III β-tubulin and to overcome paclitaxel resistance. Cancer Res 2005; 65:2397-405; PMID:15781655; http://dx.doi.org/10.1158/0008-5472.CAN-04-3065
14. Elie-Caille C, Severin F, Helenius J, Howard J, Muller DJ, Hyman AA. Straight GDP-tubulin protofilaments form in the presence of taxol. Curr Biol 2007; 17:1765-70; PMID:17919908; http://dx.doi.org/10.1016/j.cub.2007.08.063
15. Ojeda-Lopez MA, Needleman DJ, Song C, Ginsburg A, Kohl PA, Li Y, Miller HP, Wilson L, Raviv U, Choi MC. Transformation of taxol-stabilized microtubules into inverted tubulin tubules triggered by a tubulin conformation switch. Nat Mater 2014; 13:195-203; PMID:24441880; http://dx.doi.org/10.1038/nmat3858
16. Kaverina I, Straube A. Regulation of cell migration by dynamic microtubules. Semin Cell Dev Biol 2011; 22:968-74; PMID:22001384; http://dx.doi.org/10.1016/j.semcdb.2011.09.017
17. Schiff PB, Horwitz SB. Taxol stabilizes microtubules in mouse fibroblast cells. Proc Natl Acad Sci 1980; 77:1561-5; PMID:6103535; http://dx.doi.org/10.1073/pnas.77.3.1561
18. Jones DH, Nakashima T, Sanchez OH, Kozieradzki I, Komarova SV, Sarosi I, Morony S, Rubin E, Sarao R, Hojilla CV. Regulation of cancer cell migration and bone metastasis by RANKL. Nature 2006; 440:692-6; PMID:16572175; http://dx.doi.org/10.1038/nature04524
19. Halevy O, Genin O, Barzilai-Tutsch H, Pima Y, Levi O, Moshe I, Pines M. Inhibition of muscle fibrosis and improvement of muscle histopathology in dysferlin knock-out mice treated with halofuginone. Histol Histopathol 2013; 28:211-26; PMID:23275304